Z. Phys. C – Particles and Fields 36, 349–361 (1987)

Zeitschrift für Physik C Particles and Fields

A study of energy-energy correlations between 12 and 46.8 GeV c.m. energies

The TASSO Collaboration

W. Braunschweig, R. Gerhards, F.J. Kirschfink, H.-U. Martyn, P. Rosskamp
I. Physikalisches Institut der RWTH Aachen, D-5100 Aachen, Federal Republic of Germany[a]

B. Bock, J. Eisenmann, H.M. Fischer, H. Hartmann, E. Hilger, A. Jocksch, V. Mertens[1], R. Wedemeyer
Physikalisches Institut der Universität Bonn, D-5300 Bonn, Federal Republic of Germany[a]

B. Foster, A.J. Martin, A.J. Sephton
H.H. Wills Physics Laboratory, University of Bristol, Bristol, UK[b]

F. Barreiro[11,16], E. Bernardi, J. Chwastowski[2], Y. Eisenberg[3], A. Eskreys[4], K. Gather, H. Hultschig, K. Genser[5], P. Joos, H. Kowalski, A. Ladage, B. Löhr, D. Lüke, P. Mättig[6], A. Montag[3], D. Notz, J. Pawlak[5], E. Ronat[3], D. Trines, T. Tymieniecka[7], R. Walczak[7], G. Wolf, W. Zeuner
Deutsches Elektronen-Synchrotron DESY, D-2000 Hamburg 52, Federal Republic of Germany

H. Kolanoski
Physikalisches Institut, Universität Dortmund, D-4600 Dortmund, Federal Republic of Germany

T. Kracht, J. Krüger, E. Lohrmann, G. Poelz, K.-U. Pösnecker
II. Institut für Experimentalphysik der Universität Hamburg, D-2000 Hamburg, Federal Republic of Germany

D.M. Binnie, J.K. Sedgbeer, J. Shulman, D. Su, A.T. Watson
Department of Physics, Imperical College, London, UK[b]

A. Leites, J. del Peso, E. Ros
Universidad Autónoma de Madrid, E-28049 Madrid, Spain[c]

C. Balkwill, M.G. Bowler, P.N. Burrows, R.J. Cashmore, P. Dauncey[8], G.P. Heath, D.J. Mellor[9], P. Ratoff. I. Tomalin, J.M. Yelton
Department of Nuclear Physics, Oxford University, Oxford, UK[b]

S.L. Lloyd
Department of Physics, Queen Mary College, London, UK[b]

G.E. Forden[10], J.C. Hart, D.H. Saxon
Rutherford Appleton Laboratory, Chilton, Didcot, UK[b]

S. Brandt, M. Holder, L. Labarga[11]
Fachbereich Physik der Universität-Gesamthochschule Siegen, D-5900 Siegen, Federal Republic of Germany[a,f]

U. Karshon, G. Mikenberg, D. Revel, A. Shapira, N. Wainer, G. Yekutieli
Weizmann Institute, Rehovot, 76100 Israel[d]

G. Baranko[12], A. Caldwell[13], M. Cherney[14], J.M. Izen[9], D. Muller, S. Ritz, D. Strom, M. Takashima, E. Wicklund[15], Sau Lan Wu, G. Zobernig
Department of Physics, University of Wisconsin, Madison, WI 53706 USA

Received 22 July 1987

[1] Now at CERN, CH-1211 Geneva 23, Switzerland
[2] On leave from Institute of Nuclear Physics, PL-30055 Cracow, Poland
[3] On leave from Weizmann Institute, Rehovot 76100, Israel
[4] Now at Institute of Nuclear Physics, PL-30055 Cracow, Poland
[5] On leave from Warsaw University, PL-00681 Warsaw, Poland
[6] Now at IPP Canada, Carleton University, Ottawa, Canada
[7] Now at Warsaw University, PL-00681 Warsaw, Poland
[8] Now at Johns Hopkins University, Baltimore, MD 21218, USA
[9] Now at University of Illinois at Urbana, Champaign, Urbana, IL-61801, USA
[10] Now at SUNY Stony Brook, Stony Brook, NY 11794, USA
[11] On leave from Universidad Autónoma de Madrid, E-28049 Madrid, Spain
[12] Now at University of Colorado, Colorado, CO 80309, USA
[13] Now at Columbia University, New York, NY 10027, USA
[14] Now at Lawrence Berkeley Lab., Berkeley, CA 14720, USA
[15] Now at California Institute of Technology, Pasadena, CA 91125, USA
[16] Supported by the Alexander von Humboldt Stiftung

[a] Supported by Bundesministerium für Forschung und Technologie
[b] Supported by UK Science and Engineering Research Council
[c] Supported by CAICYT
[d] Supported by the Minerva Gesellschaft für Forschung GmbH
[e] Supported by US Dept. of Energy, contract DE-AC02-76ER000881 and by US Nat. Sci. Foundation Grant no INT-8313994 for travel
[f] Supported by a Research Grant from the Ministry of Science and Research of Northrhine-Westphalia

Abstract. We present data on energy-energy correlations (EEC) and their related asymmetry (AEEC) in e^+e^- annihilation in the centre of mass energy range $12 < W \leqq 46.8$ GeV. The energy and angular dependence of the EEC in the central region is well described by $O(\alpha_s^2)$ QCD plus a fragmentation term proportional to $1/\sqrt{s}$. Bare $O(\alpha_s^2)$ QCD reproduces our data for the large angle region of the AEEC. Non-perturbative effects for the latter are estimated with the help of fragmentation models. From various analyses using different approximations, we find that values for $\Lambda_{\overline{MS}}$ in the range 0.1–0.3 GeV give a good description of the data. We also compare analytical calculations in QCD for the EEC in the back-to-back region to our data. The theoretical predictions describe well both the angular and energy dependence of the data in the back-to-back region.

I Introduction

The energy-energy correlation (EEC) is a measurement of the energy flow into two calorimeter cells subtending solid angles $d\Omega$ and $d\Omega'$. Of particular interest is the average EEC [1] obtained by integrating over their orientations but keeping the angle χ between them fixed i.e.

$$\frac{1}{\sigma}\frac{d\Sigma^c}{d\cos\chi}=\frac{1}{\sigma}\sum\int\frac{\sigma}{dx_i\,dx_j\,d\cos\chi}x_i x_j\,dx_i\,dx_j \tag{1}$$

where the sum runs over all possible pairs of particles in a given final state and $x_i=E_i/\sqrt{s}$ is the fractional energy carried away by the i^{th} particle. Because of the weighting procedure in (1), the energy-energy correlation is infra-red finite outside the region $\chi=0,\pi$. Measurement of $d\Sigma/d\chi$ does not involve any ad hoc jet definition or isolation of specific event topologies which are difficult to incorporate into the theoretical description.

QCD predicts that at sufficiently high energies the correlation around 90° is dominated by single hard gluon bremsstrahlung and is therefore proportional to the quark-gluon coupling constant α_s [1]. The effects of gluon emission are enhanced, and those of fragmentation are minimized in the forward-backward asymmetry (AEEC)

$$\frac{d\Sigma^A}{d\cos\chi}=\frac{d\Sigma^c(\pi-\chi)}{d\cos\chi}-\frac{d\Sigma^c(\chi)}{d\cos\chi}. \tag{2}$$

In the lowest non-trivial order, the perturbative calculation yields [1]

$$\frac{1}{\sigma_0}\frac{d\Sigma^c}{d\cos\chi}=\frac{\alpha_s}{\pi}F(\chi), \tag{3a}$$

$$\frac{1}{\sigma_0}\frac{d\Sigma^A}{d\cos\chi}=\frac{\alpha_s}{\pi}A(\chi)=\frac{\alpha_s}{\pi}[F(\pi-\chi)-F(\chi)]. \tag{3b}$$

$F(\chi)$ being a function containing the angular dependence, while the energy dependence is implicit in the variation of the strong coupling constant.

Second order corrections have been calculated by two groups independently [2, 3]. Their results can be summarized as follows

$$\frac{1}{\sigma}\frac{d\Sigma^c}{d\cos\chi}=\frac{\alpha_s}{\pi}F(\chi)\left[1+\frac{\alpha_s}{\pi}R_{\text{corr}}(\chi)\right], \tag{4a}$$

$$\frac{1}{\sigma}\frac{d\Sigma^A}{d\cos\chi}=\frac{\alpha_s}{\pi}A(\chi)\left[1+\frac{\alpha_s}{\pi}R_{\text{asy}}(\chi)\right]. \tag{4b}$$

The values for R_{corr} and R_{asy} measure the importance of second order corrections. Note that $R_{\text{corr}}(\chi)\sim 10$, $R_{\text{asy}}\sim 3$ [2, 3] so that the perturbative expansion converges for the asymmetry faster than for any other jet measure investigated by us so far.

In order to investigate the sensitivity of the EEC to soft radiation, rather than integrating between $0<x_i<1/2$ in Eq. (1), one restricts the available phase space to $\varepsilon<x_i<1/2$ [4]. This results in a change of $F(\chi)$ as a function of the energy resolution parameter ε given by [5]

$$F(\chi,\varepsilon)=F(\chi)-\frac{2}{3}\varepsilon\frac{1}{\xi(1-\xi)}+\frac{1}{6}\varepsilon^2\frac{3-2\xi}{\xi(1-\xi)};$$
$$\xi=\tfrac{1}{2}(1-\cos\chi). \tag{5}$$

The term proportional to ε is symmetric under the exchange $\chi\to\pi-\chi$ (Or equivalently $\xi\to 1-\xi$). Therefore the corresponding function for the asymmetry has the following dependence on ε

$$A(\chi,\varepsilon)=A(\chi)+O(\varepsilon^2). \tag{6}$$

Power corrections of a perturbative nature affecting the AEEC are quadratic and not linear in the energy resolution parameter ε. These results are only slightly changed if $O(\alpha_s^2)$ effects are included [5]. Because of the infra-red stability exhibited by the AEEC, we expect it in addition to be weekly sensitive to fragmentation effects.

The above properties of the EEC and AEEC in the central angle region ($30°\lesssim\chi\lesssim 150°$) make them better suited to test low order perturbative QCD than any other known jet measure. Several experimental

studies have been published [8, 10, 11] making both qualitative and quantitative tests of QCD by using the EEC and its asymmetry. In recent years, PETRA has provided luminosity in an energy range larger than that used in previous published analyses. An experimental study of the behaviour of the EEC and AEEC in the total energy range now available and a study of fragmentation effects in the highest energy reached so far in e^+e^- annihilations, seem to us of great interest as a further test of the validity of QCD.

Up to now we have discussed the EEC and AEEC in the central angular region as a means for testing low order perturbative QCD. The regions near $\chi=0$ and $\chi=\pi$, where soft multiple gluon radiation is important, can also be used to test QCD to all orders.

It has been shown that the EEC also offers, in principle, the possibility of testing higher order QCD effects, by looking at angles $\chi\approx 0$ where calculations in the leading logarithmic approximation (LLA) were performed [6] and $\chi\approx\pi$, where results were obtained [7] based on the double logarithmic approximation.

The experimental work done in this field by the PLUTO and CELLO collaborations [8] has shown that at energies presently available quantitative comparisons between data and theory are difficult. New calculations by Collins and Soper, making use of renormalization group techniques to obtain approximate results at all order in perturbation theory [9], have renewed interest in the EEC for the back-to-back configuration ($\chi=\pi$). We have therefore analyzed our data accordingly.

II The data

The experiment was performed with the TASSO detector at PETRA. Details of the detector can be found elsewhere [12]. The data used for this analysis were taken in the period 1980–1986 at 8 c.m. energies in the range $12\leqq\sqrt{s}\leqq 46.8$ GeV (see Table 1). The bulk of the data is centred at $\sqrt{s}=14$, 22, 34.8 and 43.5 GeV c.m. energies. Hadronic final states from e^+e^- annihilation were selected using the information on charged particle momenta measured in the central detector. The selection criteria for charged particles and for multihadron events are described in [13]. Basically, a charged track has to have a momentum component transverse to the beam of $p_{xy}>0.1$ GeV and a cosine of the polar angle of $|\cos\theta|<0.87$. The r.m.s. momentum resolution including multiple scattering is $\sigma_p/p=0.016(1+p^2)^{1/2}$, with p in GeV. The main criterion for multihadron events is based on the momentum sum of the accepted charged particles, $\sum_j p_j>0.265(2E_{\text{beam}})$.

Only charged particles were used in the analysis.

Table 1. Number of events and energy range of the data samples used in this analysis

W-range (GeV)	$\langle W\rangle$ (GeV)	No. of events
11.6–12.4	12	186
12.4–14.4	14	2704
21 –23	22	1913
24 –26	25	231
29 –32	30.5	867
32 –35.2	34.8	52118
35.2–38.4	37.5	3035
38.4–46.8	43.5	6434

The EEC was determined uing the following formula:

$$\frac{1}{N_{\text{events}}}\sum_{\text{events}}\sum_{i,j}x_i x_j\delta(\cos\chi_{ij}-\cos\chi) \tag{7}$$

where $x_i=E_i/\sum_j E_j$ and E_i has been calculated assuming the particle to be a pion.

The data were corrected for initial state radiation, selection criteria, neutrals and detector effects using standard Monte Carlo techniques [13]. In the central angular region, the correction factors for the EEC are close to unity for the lower energy data samples, decreasing to around 0.9 for that at 43.5 GeV. The back-to-back region is more affected by initial state radiation and detector effects than the central region. The correction factor is large (around 1.8) near $\chi=180°$ falling off sharply as χ decreases (around 1.1 at $\chi=155°$).

We have studied the influence of the correction procedure on the final results. In particular we have investigated how the corrected data is affected by:
- cuts applied on the raw data,
- differences in the fragmentation models used for calculating the correction factors,
- differences in the values of the parameters (including Λ) used in the fragmentation models.

We estimate the uncertainties on the measurement of the EEC and the AEEC to be below 10%.

III Results

III.a The EEC *in the central region*

We show in Fig. 1 the corrected EEC distributions at 14, 22, 34.8 and 43.5 GeV. The numerical values are given in Table 2 (in intervals of $\cos\chi$) and Table 3 (in intervals of χ). The drop with energy of the central plateau, in contrast to the slow logarithmic behaviour expected in perturbation theory (3, 4), indicates a substantial fragmentation contribution to the EEC. To take it into account we use the following parametrisation [1] derived in the context of a parton model

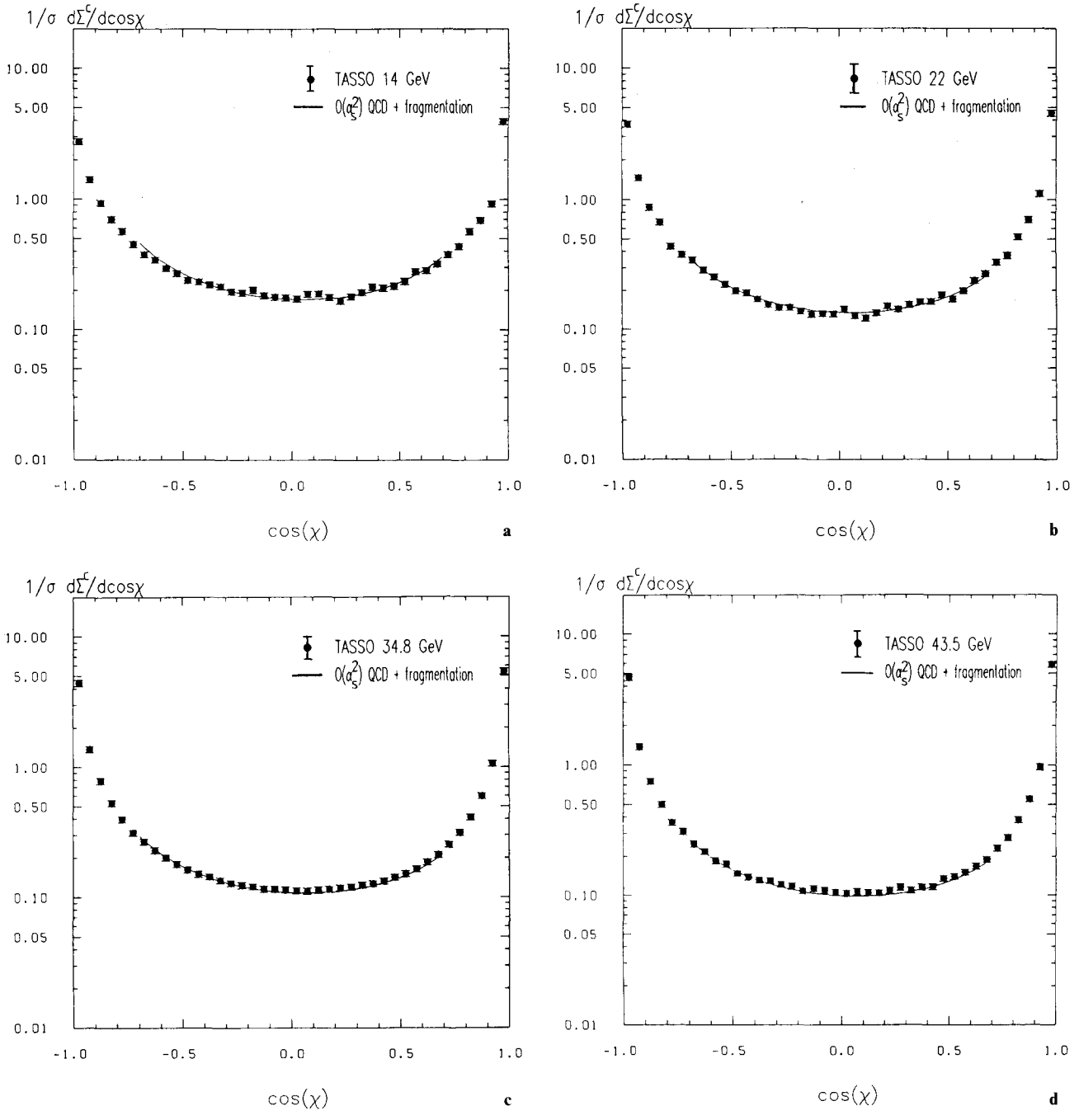

Fig. 1a–d. Corrected EEC at 14(**a**), 22(**b**), 34.8(**c**) and 43.5(**d**) GeV c.m. energies. The solid line represents the result of a fit to the sum of the $O(\alpha_s^2)$ QCD prediction and a fragmentation term

with energy independent average transverse momentum $\langle p_T \rangle$ and an energy dependence of the average multiplicity of the form $\langle n \rangle = B + C \ln(\sqrt{s})$

$$\left(\frac{d\Sigma^c}{d\cos\chi}\right)_{\text{frag.}} = \frac{C\langle p_T \rangle}{\sqrt{s}\sin^3\chi}. \tag{8}$$

This parametrisation is in agreement with Monte Carlo calculations for the energy and angular dependence of the two-jet contributions in the central angle region [5]. In Fig. 1 we see that a linear sum of the $O(\alpha_s^2)$ QCD term given by Eq. (4a) and the simple fragmentation term (8) is enough to describe the energy and angular dependence of our data, provided we

Table 2. Corrected EEC at 14, 22, 34.8 and 43.5 GeV c.m. energies (in intervals of $\cos\chi$)

$\cos\chi$ range	EEC			
	14 GeV	22 GeV	34.8 GeV	43.5 GeV
−1.00 to −0.95	2.741 ± 0.051	3.719 ± 0.077	4.410 ± 0.019	4.643 ± 0.060
−0.95 to −0.90	1.407 ± 0.019	1.463 ± 0.035	1.374 ± 0.009	1.334 ± 0.024
−0.90 to −0.85	0.933 ± 0.017	0.872 ± 0.020	0.786 ± 0.003	0.744 ± 0.008
−0.85 to −0.80	0.700 ± 0.015	0.674 ± 0.013	0.531 ± 0.002	0.495 ± 0.007
−0.80 to −0.75	0.566 ± 0.014	0.438 ± 0.011	0.399 ± 0.002	0.362 ± 0.006
−0.75 to −0.70	0.451 ± 0.013	0.378 ± 0.011	0.314 ± 0.002	0.309 ± 0.006
−0.70 to −0.65	0.376 ± 0.011	0.346 ± 0.011	0.267 ± 0.002	0.250 ± 0.006
−0.65 to −0.60	0.341 ± 0.011	0.289 ± 0.010	0.228 ± 0.002	0.219 ± 0.006
−0.60 to −0.55	0.294 ± 0.010	0.256 ± 0.010	0.200 ± 0.002	0.185 ± 0.005
−0.55 to −0.50	0.269 ± 0.009	0.223 ± 0.009	0.179 ± 0.002	0.174 ± 0.005
−0.50 to −0.45	0.238 ± 0.009	0.198 ± 0.008	0.162 ± 0.002	0.147 ± 0.005
−0.45 to −0.40	0.232 ± 0.008	0.191 ± 0.008	0.150 ± 0.002	0.138 ± 0.005
−0.40 to −0.35	0.220 ± 0.008	0.171 ± 0.007	0.143 ± 0.002	0.130 ± 0.004
−0.35 to −0.30	0.213 ± 0.008	0.155 ± 0.007	0.135 ± 0.001	0.128 ± 0.005
−0.30 to −0.25	0.195 ± 0.007	0.147 ± 0.007	0.128 ± 0.001	0.120 ± 0.004
−0.25 to −0.20	0.191 ± 0.008	0.147 ± 0.007	0.123 ± 0.001	0.116 ± 0.004
−0.20 to −0.15	0.201 ± 0.008	0.137 ± 0.007	0.120 ± 0.001	0.107 ± 0.004
−0.15 to −0.10	0.183 ± 0.007	0.130 ± 0.006	0.115 ± 0.001	0.112 ± 0.004
−0.10 to −0.05	0.178 ± 0.007	0.132 ± 0.006	0.115 ± 0.001	0.109 ± 0.004
−0.05 to 0.00	0.175 ± 0.007	0.131 ± 0.006	0.114 ± 0.001	0.105 ± 0.004
0.00 to 0.05	0.172 ± 0.007	0.143 ± 0.007	0.112 ± 0.001	0.103 ± 0.004
0.05 to 0.10	0.186 ± 0.007	0.127 ± 0.006	0.111 ± 0.001	0.106 ± 0.004
0.10 to 0.15	0.187 ± 0.007	0.121 ± 0.006	0.113 ± 0.001	0.105 ± 0.004
0.15 to 0.20	0.176 ± 0.007	0.133 ± 0.006	0.115 ± 0.001	0.104 ± 0.004
0.20 to 0.25	0.167 ± 0.006	0.151 ± 0.007	0.118 ± 0.001	0.108 ± 0.004
0.25 to 0.30	0.180 ± 0.007	0.142 ± 0.006	0.120 ± 0.001	0.115 ± 0.004
0.30 to 0.35	0.194 ± 0.007	0.154 ± 0.006	0.124 ± 0.001	0.108 ± 0.004
0.35 to 0.40	0.213 ± 0.008	0.162 ± 0.006	0.127 ± 0.001	0.115 ± 0.004
0.40 to 0.45	0.209 ± 0.008	0.164 ± 0.006	0.133 ± 0.001	0.116 ± 0.004
0.45 to 0.50	0.216 ± 0.008	0.184 ± 0.008	0.142 ± 0.001	0.134 ± 0.004
0.50 to 0.55	0.234 ± 0.008	0.171 ± 0.006	0.151 ± 0.001	0.139 ± 0.004
0.55 to 0.60	0.278 ± 0.009	0.197 ± 0.007	0.164 ± 0.001	0.150 ± 0.004
0.60 to 0.65	0.284 ± 0.009	0.238 ± 0.008	0.186 ± 0.002	0.168 ± 0.004
0.65 to 0.70	0.318 ± 0.010	0.269 ± 0.009	0.210 ± 0.002	0.189 ± 0.005
0.70 to 0.75	0.377 ± 0.011	0.329 ± 0.009	0.252 ± 0.002	0.231 ± 0.006
0.75 to 0.80	0.437 ± 0.012	0.370 ± 0.009	0.313 ± 0.002	0.278 ± 0.006
0.80 to 0.85	0.565 ± 0.014	0.516 ± 0.010	0.412 ± 0.002	0.379 ± 0.006
0.85 to 0.90	0.689 ± 0.014	0.700 ± 0.010	0.597 ± 0.003	0.546 ± 0.010
0.90 to 0.95	0.922 ± 0.017	1.104 ± 0.013	1.061 ± 0.006	0.966 ± 0.016
0.95 to 1.00	3.919 ± 0.054	4.492 ± 0.070	5.384 ± 0.020	5.838 ± 0.069

stay away from the regions near $\chi=0, \pi$, limiting ourselves to $|\cos\chi|<0.7$. The values of the two parameters obtained from the fit are $\Lambda_{\overline{MS}}=0.325\pm0.025$ GeV and $C\langle p_T\rangle=0.86\pm0.05$ GeV. Near $\chi=0, \pi$ multiple soft gluon radiation becomes important and a different treatment is necessary. Assuming the parametrisation in (8) to be realistic, the fact that the perturbative expansion for the EEC does not converge fast enough because it still could get appreciable contribution from higher orders, would imply that the value for $\Lambda_{\overline{MS}}$ obtained above can be considered an upper limit for the true value of $\Lambda_{\overline{MS}}$.

To display the drop of the central plateau of the EEC with the energy, we have plotted in Fig. 2 the EEC data integrated over the region $60°<\chi<120°$ as a function of energy. The solid line represents the prediction of $O(\alpha_s^2)$ QCD plus fragmentation term (8) which describes the data well. The broken line indicates the contribution of QCD alone. The curves approach each other as the energy increases. We are aware of the fact that the approach adopted is naive and limited in scope. It serves however to get an estimate of the fragmentation contribution to the EEC. It also illustrates that in order to describe the central angle behaviour of our EEC data, in addition to the perturbative results only a two-jet fragmentation term is needed.

In Fig. 3 we present the AEEC as a function of $\cos\chi$ for 4 different energies. In contrast to the behaviour exhibited by the EEC, the asymmetry varies very

Table 3. Corrected EEC at 14, 22, 34.8 and 43.5 GeV c.m. energies (in intervals of χ)

χ range	EEC			
	14 GeV	22 GeV	34.8 GeV	43.5 GeV
0.0 to 3.6	66.27 ±1.075	61.07 ±1.201	60.19 ±0.316	62.87 ±0.824
3.6 to 7.2	1.620±0.099	3.025±0.153	5.752±0.071	7.522±0.205
7.2 to 10.8	1.450±0.067	2.706±0.097	4.104±0.036	4.620±0.086
10.8 to 14.4	1.385±0.054	2.201±0.068	2.856±0.023	2.619±0.049
14.4 to 18.0	1.183±0.043	1.671±0.047	1.911±0.015	1.840±0.029
18.0 to 21.6	0.988±0.033	1.342±0.038	1.318±0.010	1.204±0.020
21.6 to 25.2	0.899±0.027	0.976±0.027	0.937±0.007	0.839±0.016
25.2 to 28.8	0.740±0.023	0.797±0.021	0.691±0.005	0.621±0.010
28.8 to 32.4	0.653±0.019	0.606±0.017	0.526±0.004	0.481±0.008
32.4 to 36.0	0.568±0.017	0.532±0.015	0.413±0.003	0.376±0.007
36.0 to 39.6	0.483±0.015	0.391±0.012	0.334±0.003	0.301±0.006
39.6 to 43.2	0.382±0.012	0.356±0.010	0.276±0.003	0.246±0.005
43.2 to 46.8	0.352±0.011	0.298±0.009	0.239±0.002	0.213±0.005
46.8 to 50.4	0.312±0.010	0.257±0.009	0.201±0.002	0.186±0.004
50.4 to 54.0	0.288±0.009	0.235±0.008	0.179±0.002	0.164±0.004
54.0 to 57.6	0.265±0.009	0.187±0.006	0.158±0.002	0.146±0.004
57.6 to 61.2	0.232±0.008	0.178±0.006	0.147±0.001	0.144±0.004
61.2 to 64.8	0.211±0.007	0.180±0.007	0.137±0.001	0.127±0.003
64.8 to 68.4	0.212±0.007	0.159±0.006	0.129±0.001	0.122±0.003
68.4 to 72.0	0.201±0.007	0.153±0.006	0.122±0.001	0.117±0.004
72.0 to 75.6	0.179±0.006	0.148±0.006	0.117±0.001	0.113±0.003
75.6 to 79.2	0.170±0.006	0.151±0.006	0.114±0.001	0.112±0.004
79.2 to 82.8	0.179±0.006	0.132±0.006	0.112±0.001	0.109±0.004
82.8 to 86.4	0.187±0.006	0.121±0.005	0.110±0.001	0.106±0.004
86.4 to 90.0	0.179±0.006	0.141±0.006	0.111±0.001	0.105±0.003
90.0 to 93.6	0.177±0.006	0.132±0.005	0.111±0.001	0.108±0.003
93.6 to 97.2	0.177±0.006	0.130±0.005	0.113±0.001	0.111±0.004
97.2 to 100.8	0.201±0.007	0.140±0.005	0.116±0.001	0.116±0.004
100.8 to 104.4	0.191±0.007	0.143±0.006	0.120±0.001	0.116±0.004
104.4 to 108.0	0.194±0.006	0.151±0.006	0.127±0.001	0.121±0.004
108.0 to 111.6	0.221±0.007	0.156±0.006	0.132±0.001	0.129±0.004
111.6 to 115.2	0.226±0.007	0.177±0.007	0.145±0.001	0.137±0.004
115.2 to 118.8	0.234±0.008	0.208±0.008	0.155±0.002	0.153±0.004
118.8 to 122.4	0.264±0.008	0.198±0.008	0.168±0.002	0.169±0.005
122.4 to 126.0	0.284±0.009	0.268±0.010	0.190±0.002	0.185±0.005
126.0 to 129.6	0.335±0.011	0.277±0.009	0.217±0.002	0.212±0.006
129.6 to 133.2	0.365±0.011	0.326±0.011	0.255±0.003	0.243±0.006
133.2 to 136.8	0.428±0.013	0.353±0.012	0.294±0.003	0.278±0.007
136.8 to 140.4	0.496±0.014	0.413±0.013	0.347±0.003	0.339±0.008
140.4 to 144.0	0.595±0.016	0.477±0.014	0.432±0.004	0.401±0.008
144.0 to 147.6	0.696±0.019	0.716±0.020	0.537±0.005	0.491±0.010
147.6 to 151.2	0.884±0.024	0.755±0.020	0.697±0.006	0.661±0.012
151.2 to 154.8	0.989±0.028	1.004±0.028	0.890±0.007	0.859±0.015
154.8 to 158.4	1.292±0.036	1.294±0.033	1.227±0.009	1.149±0.019
158.4 to 162.0	1.617±0.046	1.747±0.047	1.694±0.012	1.657±0.028
162.0 to 165.6	1.923±0.059	2.291±0.064	2.443±0.018	2.439±0.040
165.6 to 169.2	2.649±0.096	3.230±0.097	3.631±0.027	3.640±0.062
169.2 to 172.8	3.133±0.123	4.536±0.155	5.566±0.047	5.734±0.113
172.8 to 176.4	3.949±0.210	5.893±0.276	8.011±0.089	8.984±0.237
176.4 to 180.0	5.060±0.506	8.406±0.712	12.173±0.222	13.264±0.651

slowly with c.m. energy. In fact the solid line was obtained by a simultaneous fit of the $O(\alpha_s^2)$ QCD predictions (4b) to all 4 distributions in the region $\cos\chi < 0.75$. For the only free parameter in this fit we obtain $\Lambda_{\overline{MS}} = 0.125 \pm 0.022$ GeV. The fact that the QCD prediction does not describe the data at $\cos\chi$ near 1 is expected since this is the region dominated by multiple soft gluon bremsstrahlung effects.

We have plotted in Fig. 4 the AEEC data integrated over the region $\cos\chi < 0.75$. The integrated asymmetry exhibits a variation with c.m. energy consistent with the logarithmic behaviour of $O(\alpha_s^2)$ QCD (solid line).

To gain further insight into the dependence with c.m. energy of the AEEC, we plot our data in various regions of $\cos\chi$, see Fig. 5. There is practically no

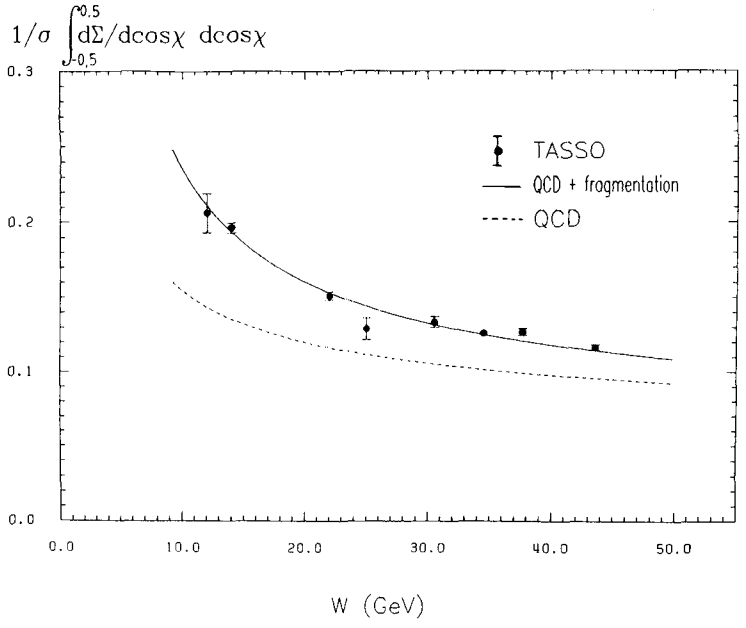

Fig. 2. Integrated EEC as a function of the energy. The solid line represents the result of a fit to the sum of the $O(\alpha_s^2)$ QCD prediction and a fragmentation term. The dashed curve is the contribution of QCD alone

energy dependence for $\cos\chi < 0.9$. For small asymmetry angles, however, we observe a strong variation with the c.m. energy, indicating the dominance of two-jet fragmentation effects.

To estimate the importance of fragmentation effectsin the AEEC for angles $30° \lesssim \chi \lesssim 150°$, we compare our data with fragmentation models. For this purpose, we concentrate on the high energy data ($38.4\ \text{GeV} \leqq W \leqq 46.8\ \text{GeV}$). A similar analysis of TASSO data at lower energies ($33\ \text{GeV} \leqq W \leqq 36.6\ \text{GeV}$) can be found in [11]. We consider both the independent fragmentation scheme of Ali et al. [14] and the string model of the Lund group [15]. Second order corrections are included as discussed in [5] using (ε, δ) cut-offs to separate two- from three- and four-jet events. In Fig. 6 both fragmentation models are compared with the AEEC data at 43.5 GeV. Both fragmentation schemes reproduce well the data over the whole angular range. Fits to the data in the region $\cos\chi < 0.9$ yield $\Lambda_{\overline{MS}} = 0.165 \pm 0.028$ GeV for independent fragmentation and $\Lambda_{\overline{MS}} = 0.305 \pm 0.045$ GeV for the string model.

In Table 4 we show the values of $\Lambda_{\overline{MS}}$ and the corresponding values of α_s at $\sqrt{s} = 43.5$ GeV obtained from the different approximations discussed so far. The systematic errors include, in addition to those from the correction procedure, other uncertainties from the choice of the (ε, δ) parameters ($\sim 4\%$) and the angular regions used in the fits ($\sim 6\%$).

The fact that using different approximations gives different values for $\Lambda_{\overline{MS}}$ deserves comment. The uncertainties in the values of $\Lambda_{\overline{MS}}$ are due to our poor knowledge of fragmentation effects. At present they are not understood from first principles. All fragmentation models giving good overall description of the gross features exhibited by multiparticle final states predict non-perturbative contributions to the AEEC to be negative [17]. Therefore the value for $\Lambda_{\overline{MS}}$ obtained from fitting the AEEC data to $O(\alpha_s^2)$ predictions should be considered as a lower limit for the true value of $\Lambda_{\overline{MS}}$. Those values obtained from a comparison of the AEEC data to the two models considered provide us with an educated guess of the uncertainties due to the detailed way in which quarks and gluons fragment. In terms of the strong coupling constant they are of order 15%, see Table 4.

Measurements of AEEC at PETRA have been carried out by the CELLO, JADE, MARK J, PLUTO and TASSO collaborations. The values of $\Lambda_{\overline{MS}}$ obtained from the above analysis can be compared with the results of the MARK J and PLUTO collaborations [10], where a similar treatment of $O(\alpha_s^2)$ corrections was used, they are in agreement with the measurement of this paper and also with our previous work at 34 GeV c.m. energy [11]. Our estimations for $\Lambda_{\overline{MS}}$ are also in agreement with those resulting from the analysis of the planar triple energy correlation (PTC) done by the MARK J collaboration [19].

III.b The EEC *in the back-to-back region*

For very small and very large angles ($\chi \approx 0$, $\chi \approx \pi$), the EEC data can not be described by low order perturbative QCD. In this angular region not only hadron formation but also multiple soft gluon emission

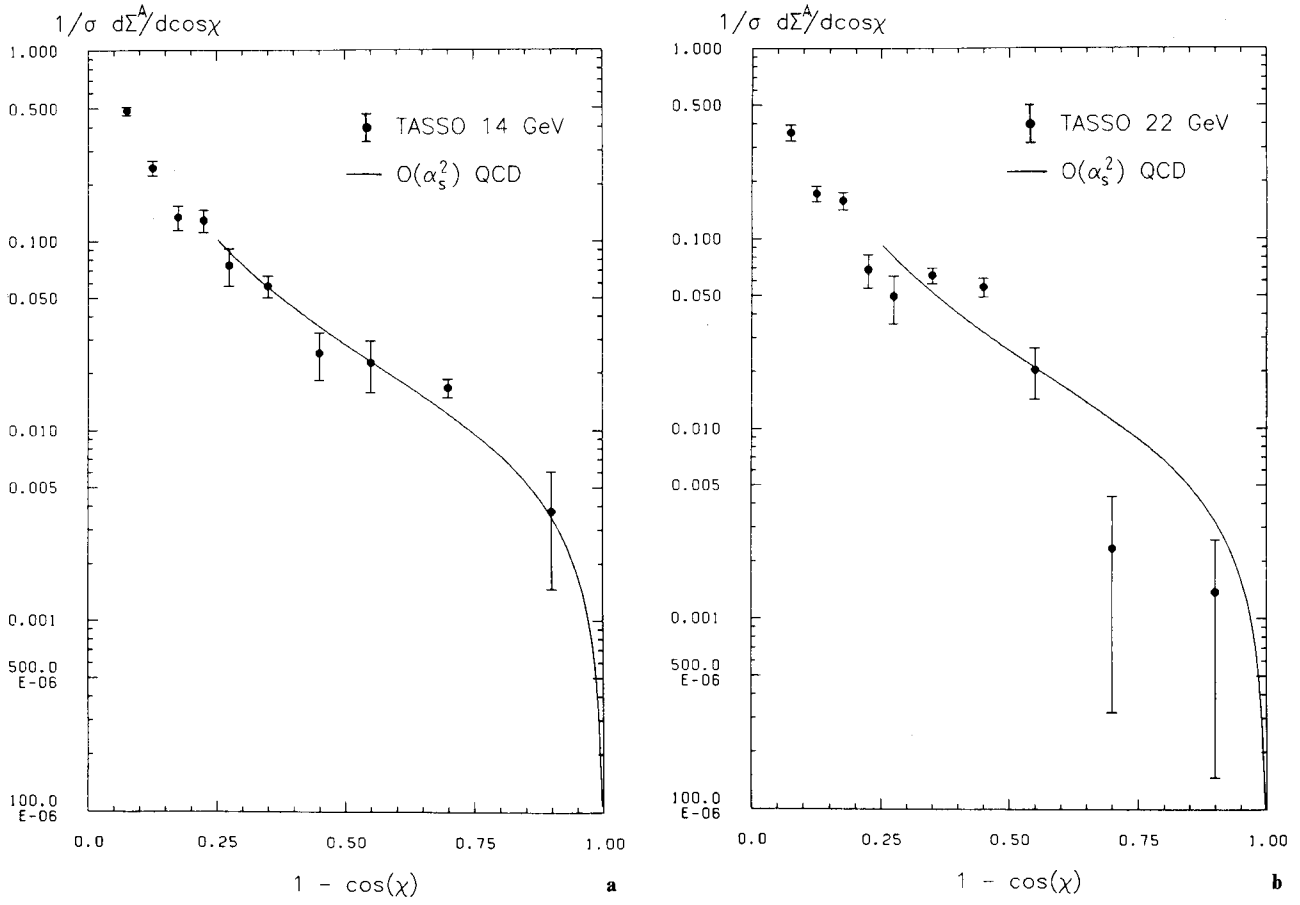

Fig. 3a–d. The AEEC at 14(**a**), 22(**b**), 34.8(**c**), 43.5(**d**) GeV c.m. energies. The solid lines represent the predictions of $O(\alpha_s^2)$ QCD for $\Lambda_{\overline{MS}}=0.125$ GeV

Table 4. Values of $\Lambda_{\overline{MS}}$ and of α_s at $\sqrt{s}=43.5$ GeV obtained from the different approximations used in the study of the AEEC. The fist error is statistical, the second systematic

Method	$\Lambda_{\overline{MS}}$ (GeV)	α_s at 44 GeV
$O(\alpha_s^2)$ QCD fitted to data at 14, 22, 34.8 and 43.5 GeV	0.125 ± 0.025	$0.123\pm0.004\pm0.011$
$O(\alpha_s^2)$ QCD + Ali et al. fragmentation fitted to data at 43.5 GeV	0.165 ± 0.028	$0.129\pm0.004\pm0.011$
$O(\alpha_s^2)$ QCD + Lund fragmentation fitted to data at 43.5 GeV	0.305 ± 0.045	$0.143\pm0.005\pm0.012$

has to be taken into account. In this section we compare our data in the back-to-back region ($\chi\approx\pi$) with approximate QCD calculations [9] for which all orders in α_s were used.

The formula for the energy-energy correlation function we use [9] is an extension to all relevant logarithms of the LLA result [7]. It contains two terms, a QCD part and a parton model correction designed to account for the fragmentation effects due to low energy final state particles (those with energy E below a certain cutoff E_0). Following [9] we call $\theta=\pi-\lambda$ the acollinearity angle between two particles ($\theta=0$ being the back-to-back configuration), and $Q=\sqrt{s}$ the total centre-of-mass energy of the annihilation process. The formula reads:

$$\frac{1}{\sigma}\frac{d\Sigma}{d\cos\theta}=\left[\frac{1}{\sigma}\frac{d\Sigma}{d\cos\theta}\right]_{\mathrm{QCD}}+2\frac{E_0}{Q}A(0)\frac{E_0^2}{\langle P_T^2\rangle}\left[f\left(\frac{E_0^2}{\langle P_T^2\rangle}\sin^2\theta\right)-f\left(\frac{E_0^2}{\langle P_T^2\rangle}4\sin^2(\theta/2)\right)\right]. \quad (9)$$

The constant $A(0)$ is defined as the $x\to0$ limit ($x=2E/Q$) of $A(x)=\Sigma_A x d_{A/a}(x;Q^2)$ where $d_{A/a}$ gives the probability that a parton of type a will decay into a hadron of type A carrying a fraction x of the

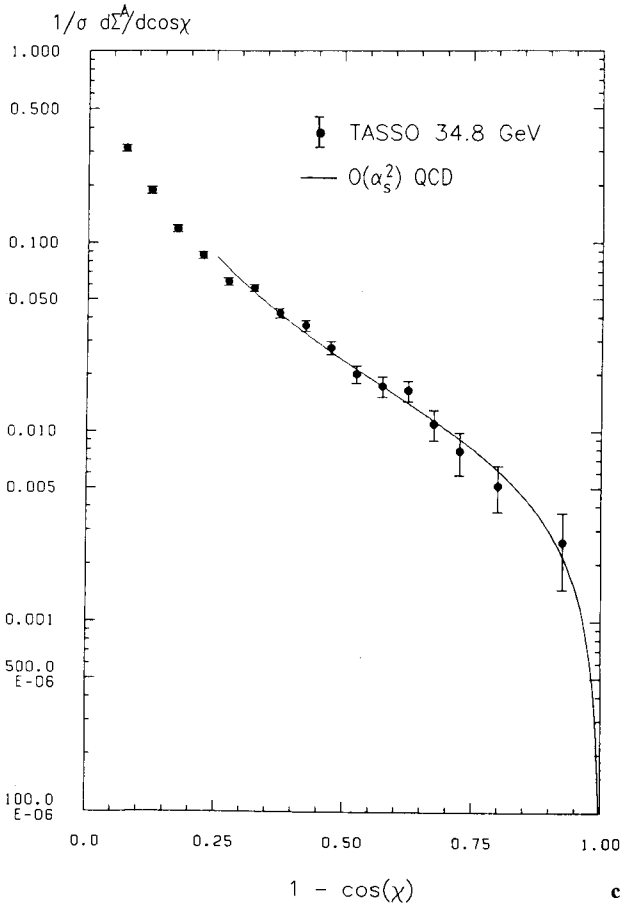

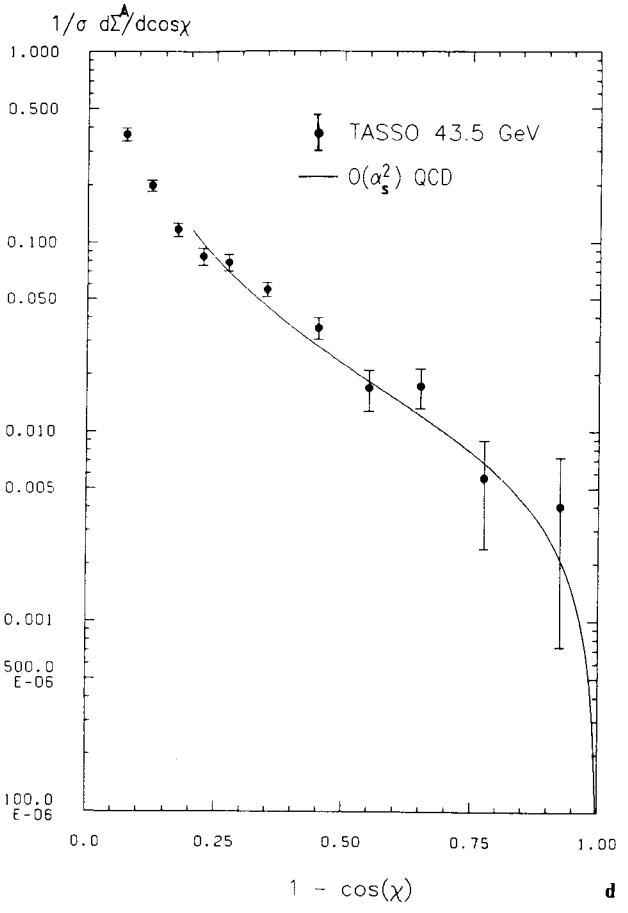

parton's momentum, and $\langle P_T^2 \rangle$ is the mean squared hadron transverse momentum with respect to the jet axis. We have used [9, 18] $A(0)=4$, $E_0=0.4$ GeV and $\langle P_T^2 \rangle = 0.45$ GeV^2. The function f is given by:

$$f(z)=z^{-\frac{3}{2}}\int_0^z y^{-\frac{1}{2}}e^{-y}\,dy. \tag{10}$$

The parton model correction is not important when Q is large or θ is small and it does not affect our analysis of the back-to-back configuration. The contribution of the low energy particles for small θ is accounted for by the QCD part.

The QCD term is further divided into two parts:

$$\left[\frac{1}{\sigma}\frac{d\Sigma}{d\cos\theta}\right]_{\mathrm{QCD}}=\frac{Q^2}{16\pi}\int d^2b\,e^{-ik_T b}\tilde{W}(b,Q)+Y(\theta,Q) \tag{11}$$

with $k_T \equiv Q\sin(\theta/2)$ [9]. The Fourier transformation in (11) will allow the separation of perturbative (and calculable) from non-perturbative QCD contributions at small θ. The first term on the right-hand side contains the soft bremsstrahlung physics and gives the dominant contribution at small θ. The function Y provides a correction so that the usual perturbative result is obtained for angles in the central region. To order α_s [9], it is the function in Eq. (3a) plus a term which cancels the divergences when $\theta \to 0$.

The function $\tilde{W}(b, Q)$ can be calculated perturbatively, but the calculation is unreliable for large values of the impact parameter b, ($b > b_{\max}$ say). In order to deal with these two regions of b, $\tilde{W}$ is written as the product of a perturbative factor and a non-perturbative one:

$$\tilde{W}(b,Q) = \tilde{W}(b_*,Q)_{\mathrm{pert}}\exp[-\ln(Q^2/Q_0^2)f_1(b)-f_2(b)] \tag{12}$$

where $b_*=b/(1+b^2/b_{\max}^2)^{1/2}$. The definition of b_* is such that $b_* < b_{\max}$ always, and $b_* \to b$ when b is small. Then $\tilde{W}(b_*, Q)_{\mathrm{pert}}$ can be reliably calculated in perturbation theory, provided that $b_{\max}$ is not too large. The value of $b_{\max}$ is otherwise arbitrary, and a change in $b_{\max}$ can be compensated by a change in the non-perturbative functions $f_1(b)$ and $f_2(b)$. From a physical point of view, the constant Q_0, which appears for dimensional reasons, is completely arbitrary. However, it is recommended [9] to take $Q_0=27$ GeV and $b_{\max}=0.5$ GeV^{-1} for the purpose of calculation.

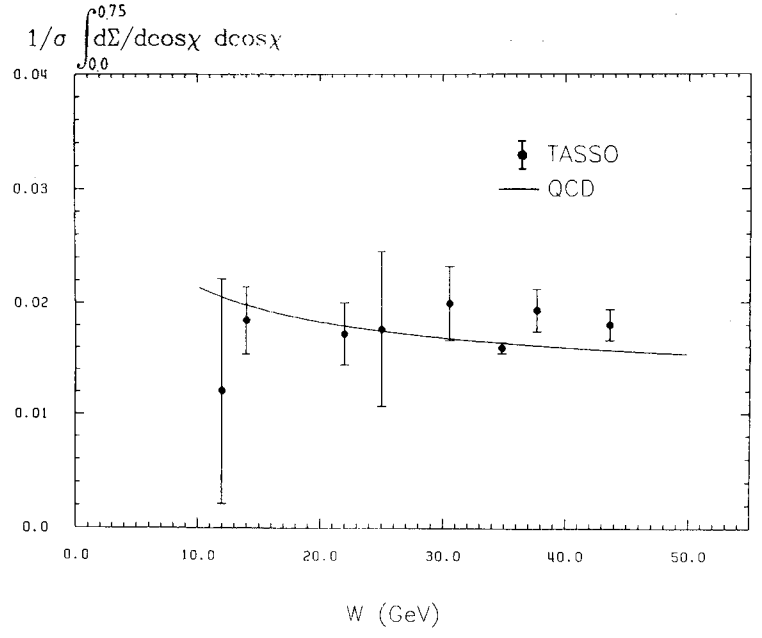

Fig. 4. Integrated AEEC as a function of the energy. The solid line is the prediction of $O(\alpha_s^2)$ QCD for $\Lambda_{\overline{MS}}=0.125$ GeV

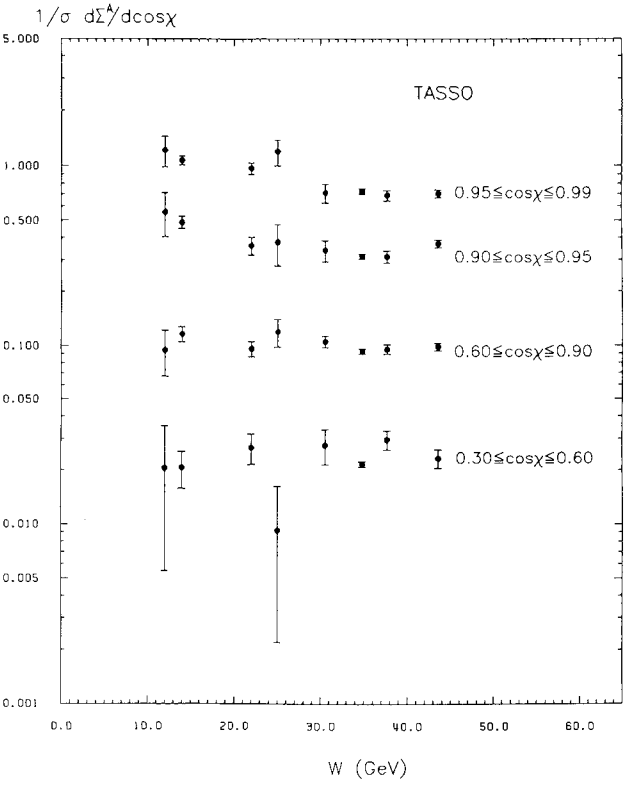

Fig. 5. Energy dependence of the AEEC integrated over different ranges of $\cos\chi$

The non-perturbative (large b) behaviour of $\tilde{W}$ in (12), is handled by the functions $f_1(b)$ and $f_2(b)$. It is not known how to compute these functions in QCD. They have to be obtained by a fit to the data, with the constraint that they must vanish for $b\to 0$.

We use the following parametrisation for f_1 and f_2 [18]:

$$f_1(b)=A_{11}b+A_{12}b^2+A_{00}\left(1-\frac{b_*}{b}\right)$$

$$f_2(b)=A_{21}b+A_{22}b^2+A_{30}\left(1-\frac{b_*}{b}\right). \tag{13}$$

Note that these two functions are energy independent: once they are extracted from the data at two different energies, they can be used to make quantitative predictions for the EEC in the back-to-back configuration at any other energy. Ideally one would like to divide up the data into a low and a high centre-of-mass energy regime, fixing f_1 and f_2 in the former, while attempting to measure the QCD scale parameter in the latter. Unfortunately the energy spanned by TASSO does not allow us to perform this task.

Therefore we have fitted the non-perturbative functions (13) appearing in (10, 11) to our data at the four energies simultaneously. The data were grouped in 3.6° θ intervals and only the small angle region $0<\theta<21.6°$ $(1-\cos\theta<0.07)$, was used in the fits. The results are shown in Fig. 7. The theoretical predictions describe well both the angular and energy dependence of the data. The fitted values of the parameters involved in $f_1(b)$ and $f_2(b)$ are:

$A_{11}=0.60\pm0.17$ GeV; $\quad A_{21}=0.94\pm0.11$ GeV;

$A_{12}=0.13\pm0.05$ GeV^2; $\quad A_{22}=0.56\pm0.04$ GeV^2;

$A_{00}=-1.02\pm0.29$; $\quad A_{30}=0.40\pm0.19$.

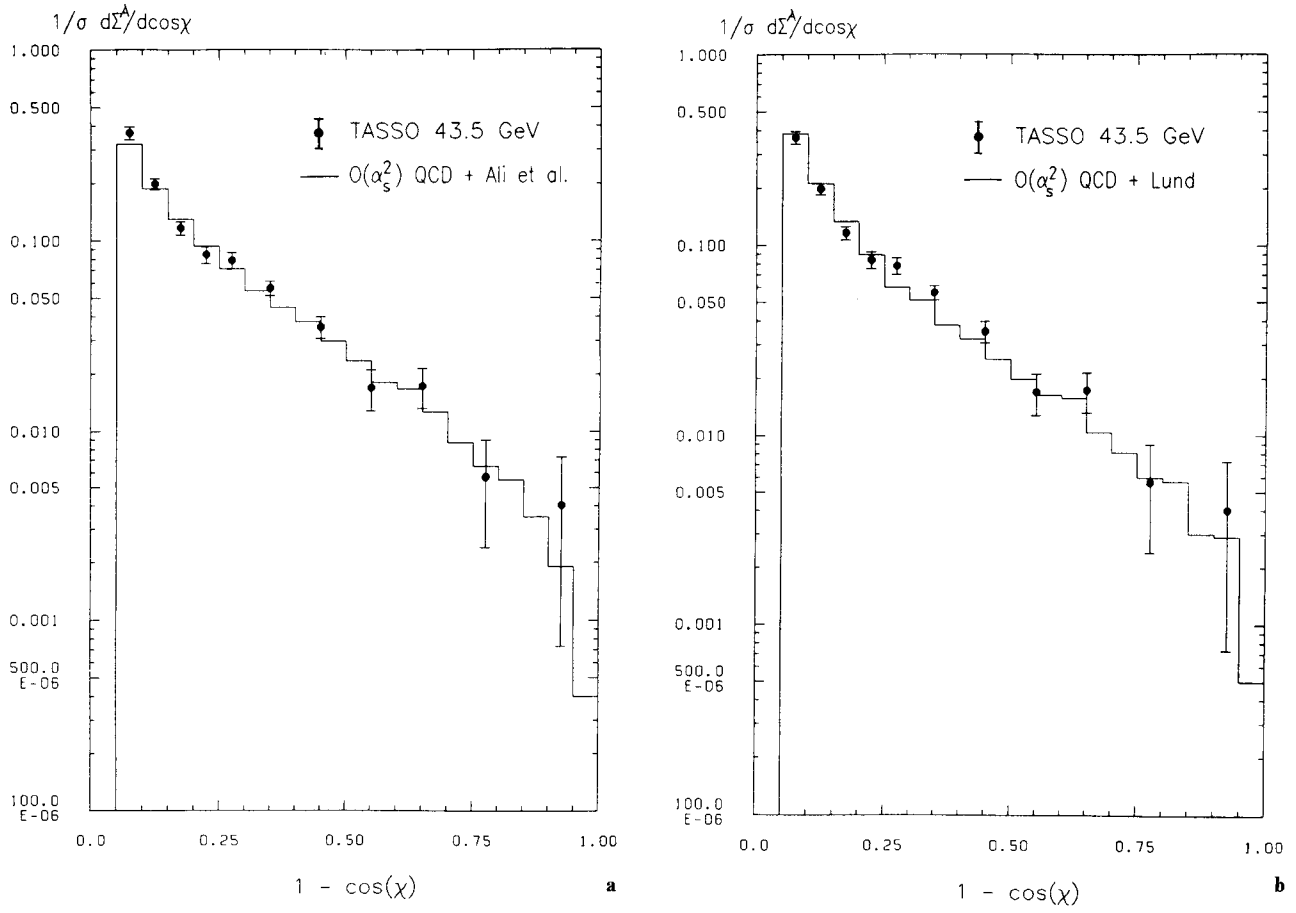

Fig. 6a, b. The AEEC at 43.5 GeV c.m. energy. The solid line represents the expectations from $O(\alpha_s^2)$ QCD and the Ali et al. (**a**) and Lund (**b**) fragmentation models

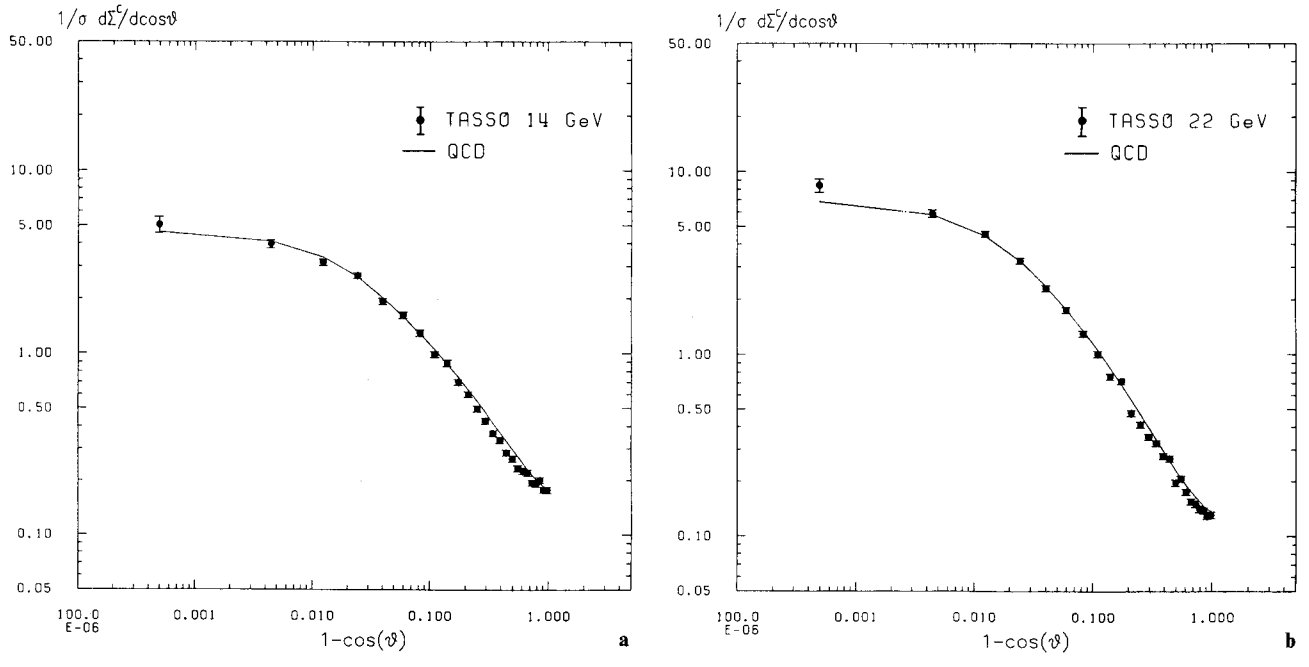

Fig. 7a–d. The EEC data in the backward hemisphere at 14(**a**), 22(**b**), 34.8(**c**) and 43.5(**d**) GeV c.m. energies. Solid curves represent the results of a fit to calculations by Collins and Soper

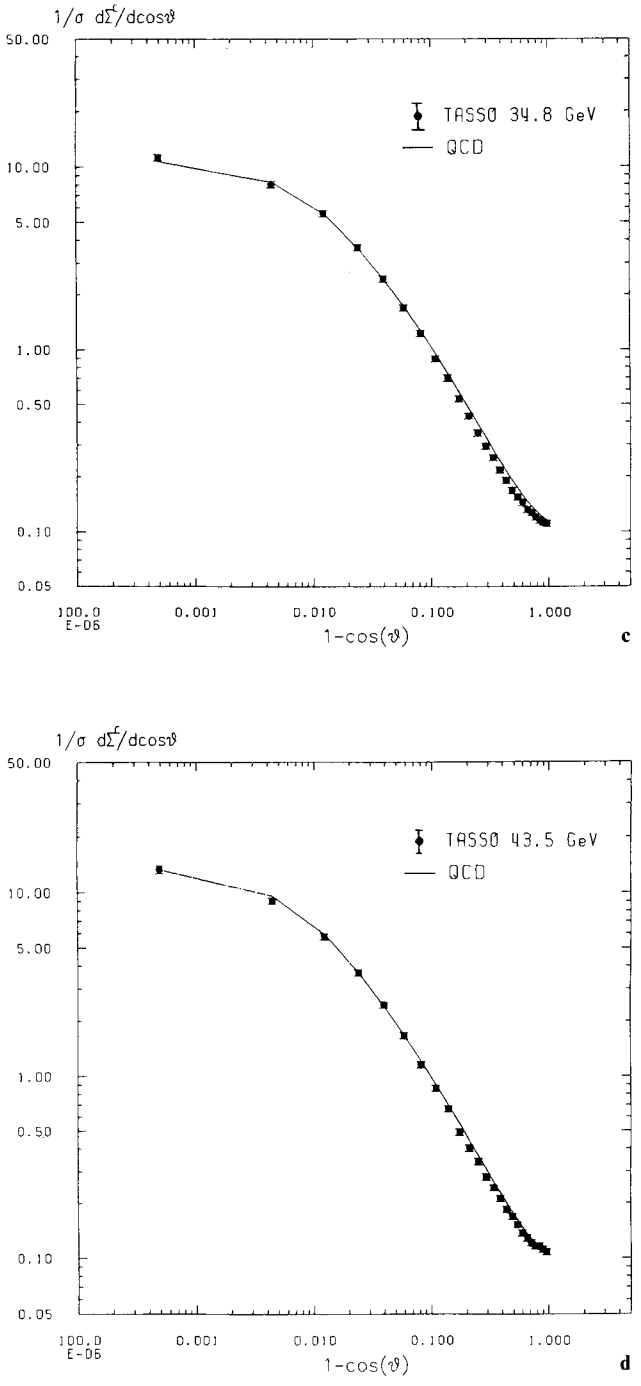

Fig. 7c, d

Note that $\Lambda_{\overline{MS}}$ was kept constant in the fit at 0.150 GeV. The effect of changing Λ is to alter the predicted cross section at higher energies. We have checked that varying the QCD scale parameter within the range discussed in the previous section, resulted in fits of comparable quality.

IV Conclusions

We have presented data on energy-energy correlations (EEC) and their asymmetry (AEEC) in e^+e^- annihilation in the centre of mass energy range $12 \leqq W \leqq 46.8$ GeV. We have seen that the AEEC is a good quantity to test low order perturbative QCD. The central angular region of the EEC is well described by QCD plus a fragmentation term proportional to $1/\sqrt{s}$. For the AEEC we observe a very mild energy dependence. The AEEC data in the large angle region can be described by QCD alone. We performed fits to the AEEC at large angles using perturbative predictions to $O(\alpha_s^2)$ QCD and also using $O(\alpha_s^2)$ predictions and fragmentation models and obtained values for $\Lambda_{\overline{MS}}$ between 0.1 and 0.3 GeV. These uncertainties are due to our lack of understanding of non-perturbative effects. Analytical calculations to all orders in QCD for the EEC for the back-to-back configuration have also been compared to our data. The theoretical predictions describe well both the angular and energy dependence of the data in the back-to-back region.

Acknowledgements. We gratefully acknowledge the support by the DESY directorate, the PETRA machine group and the DESY computer centre. Those of us from outside DESY wish to thank the DESY directorate for the hospitality extended to us while working at DESY. We would like to thank A. Ali, J. Collins and D. Soper for helpful discussions and for making available to us computer codes used in part of this analysis.

References

1. C.L. Basham, L.S. Brown, S.D. Ellis, S.T. Love: Phys. Rev. Lett. 41 (1978) 1585; Phys. Rev. D19 (1979) 2018
2. A. Ali, F. Barreiro: Phys. Lett. 118B (1982) 155
3. D. Richards, W.J. Stirling, S.D. Ellis: Phys. Lett. 119B (1982) 193
4. G. Sterman, S. Weinberg: Phys. Rev. Lett. 39 (1977) 1436
5. A. Ali, F. Barreiro: Nucl. Phys. 236B (1984) 269
6. K. Konishi, A. Ukawa, G. Veneziano: Phys. Lett. 80B (1979) 259
7. Yu.L. Dokshitzer, D.I. D'yakonov, S.I. Troyan: Phys. Lett. 78B (1978) 290; G. Parisi, R. Petronzio: Nucl. Phys. B154 (1979) 427; G. Curci, M. Greco, Y. Shrivastava: Nucl. Phys. B159 (1979) 451
8. PLUTO Collaboration, Ch. Berger et al.: Phys. Lett. 90B (1980) 312; Phys. Lett. 99B (1981) 292; CELLO Collaboration, H.J. Behrend et al.: Z. Phys. C – Particles and Fields 14 (1982) 95
9. J.C. Collins, D.E. Soper: Nucl. Phys. B193 (1981) 381; J.C. Collins, D.E. Soper: Nucl. Phys. B197 (1982) 446; J.C. Collins, D.E. Soper: Phys. Rev. Lett. 48 (1982) 655; J.C. Collins, D.E. Soper: Acta Phys. Polon B16 (1985) 1047; Oregon, Eugene OITS 273, March 85

10. CELLO Collaboration, H.J. Behrend et al.: Phys. Lett. 138 B (1984) 311; JADE Collaboration, W. Bartel et al.: Z. Phys. C – Particles and Fields 25 (1984) 231; MAC Collaboration, E. Fernandez et al.: Phys. Rev. D 31 (1985) 2724; MARK II Collaboration, D. Schlatter et al.: Phys. Rev. Lett. 49 (1982) 521; MARK J Collaboration, B. Adeva et al.: Phys. Rev. Lett. 50 (1983) 2051; Phys. Rev. Lett. 54 (1985) 1750; PLUTO Collaboration, Ch. Berger et al.: Z. Phys. C – Particles and Fields 28 (1985) 365
11. TASSO Collaboration, M. Althoff et al.: Z. Phys. C – Particles and Fields 26 (1984) 157
12. TASSO Collaboration, R. Brandelik et al.: Phys. Lett. 83 B (1979) 261; Z. Phys. C – Particles and Fields 4 (1980) 87
13. TASSO Collaboration, M. Althoff et al.: Z. Phys. C – Particles and Fields 22 (1984) 307
14. A. Ali et al.: Phys. Lett. B 93 (1980) 155; Nucl. Phys. B 168 (1980) 409
15. B. Andersson, G. Gustafson, T. Sjöstrand: Z. Phys. C – Particles and Fields 6 (1980) 235; Nucl. Phys, B 197 (1982) 45
16. J.C. Collins, D.E. Soper: Nucl. Phys. 284 B (1987) 253
17. S.D. Ellis: Phys. Lett. 117 B (1982) 333
18. J.C. Collins, D.E. Soper: ENCOR a program to fit EEC data in the back-to-back region; User's handbook
19. MARK J Collaboration, B. Adeva et al.: Phys. Lett.180 B (1986) 181